Supporting Information

ZnO Nanorods/ZnSe Heteronanostructure Arrays with a Tunable Microstructure of ZnSe Shell for Visible Light Photocatalysis

Zhengcui Wu*, Huan Wang, Yejing Xue, Baoer Li and Baoyou Geng*

Anhui Key Laboratory of Molecule-Based Materials, The Key Laboratory of Functional Molecular Solids, Ministry of Education, Center of nano science and technology, College of Chemistry and Materials Science, Anhui Normal University, Wuhu 241000, People's Republic of China

---

*To whom correspondence should be addressed.

Tel: +86-553-3869302; Fax: +86-553-3869302.

E-mail: zhengcui@mail.ahnu.edu.cn (Z. Wu), bygeng@mail.ahnu.edu.cn (B. Geng).

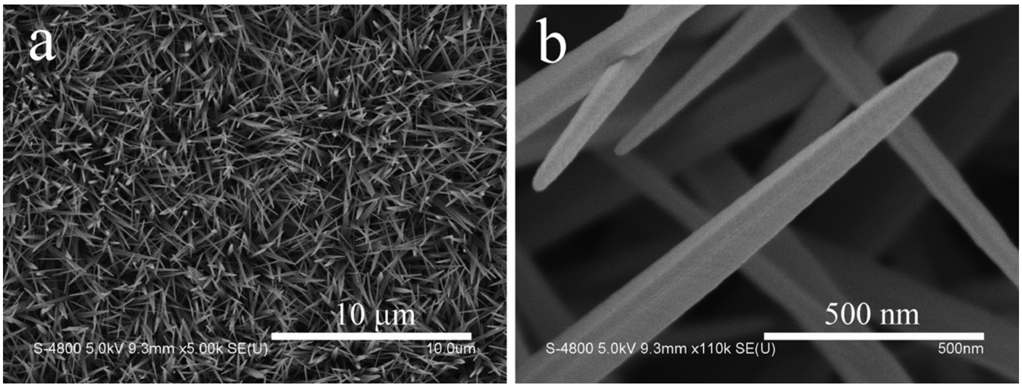

Figure S1. Low- and high-magnification FESEM images of the needle-like ZnO-NRs array on zinc foil.

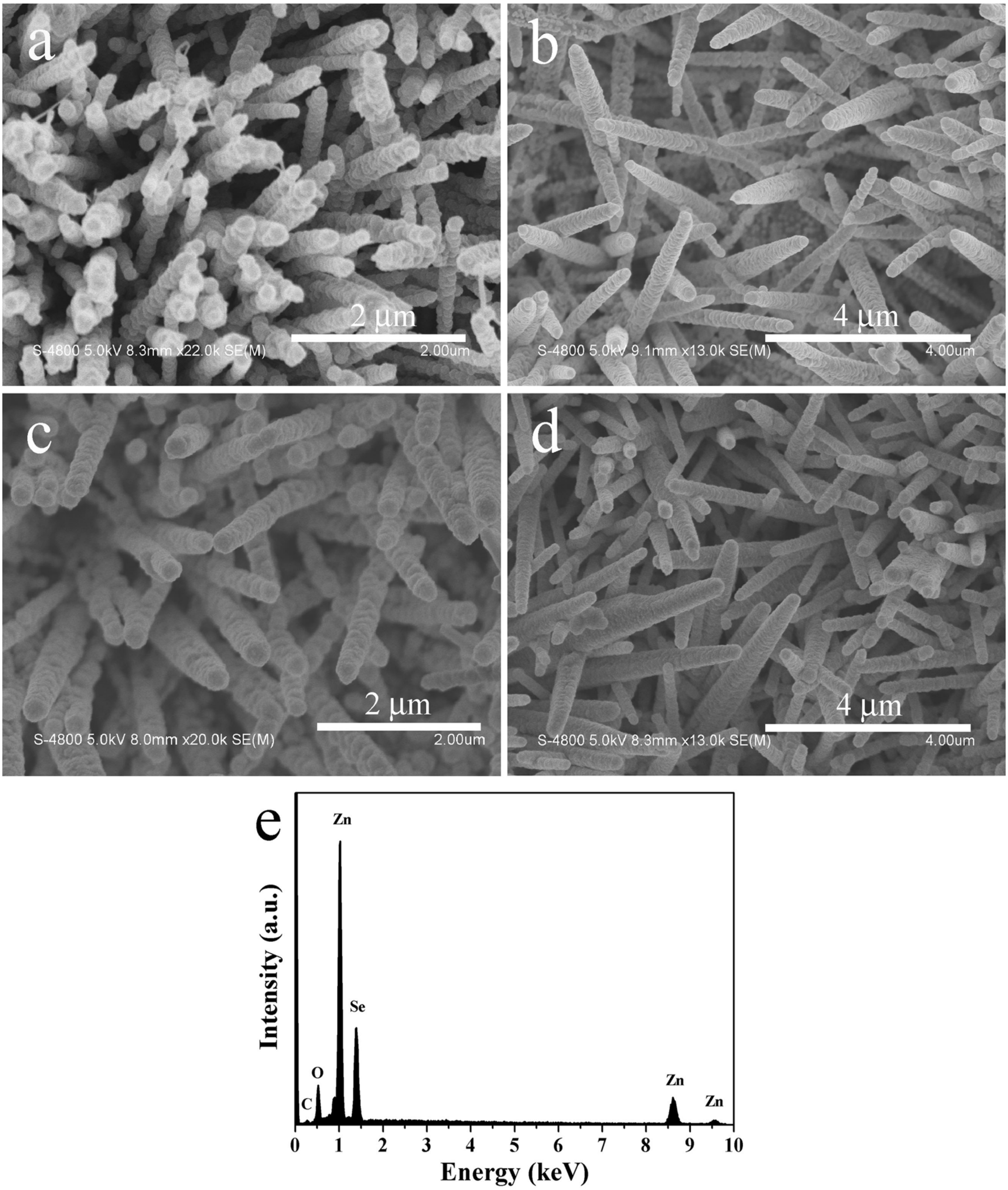

Figure S2. Typical FESEM images of the ZnO-NRs/ZnSe-NPs heterostructure array synthesized with different concentrations of $NaBH_4$, ammonia and the reaction time. (a) without $NaBH_4$; (b) with $NaBH_4$ doubled; (c) with 10 mL of ammonia; (d) with the reaction time increased to 20 h; and

(e) The corresponding EDX spectrum of the product with the reaction time of 20 h.

The investigation on the concentration of $NaBH_4$ showed the heteronanostructure with larger ZnSe nanoparticles on ZnO-NRs was obtained without $NaBH_4$ while keeping other parameters constant (Figure S2a). As the amount of $NaBH_4$ doubled, the coverage of secondary ZnSe nanoparticles on ZnO-NRs was less uniform with some coverd more and some coverd less (Figure S2b). The results indicated the size and coverage of ZnSe nanoparticles shell is relatively sensitive to $NaBH_4$ concentration, and the modest amount of $NaBH_4$ will favor for smaller ZnSe nanoparticles uniformly covered on ZnO-NRs. On the other hand, the concentration of ammonia is another crucial parameter affecting the shell nanoparticles microstructure. There was hardly ZnSe nanoparticles covered on ZnO-NRs without ammonia (image not shown). Therefore, ammonia can supply the alkaline medium for $NaBH_4$ to reduce Se power into Se^{2-} ions as well as itself promotes the dissolution of Se power. In addition, the ZnO-NRs/ZnSe-NPs heterostructure can steadily existed with ammonia increased to 10 mL (Figure S2c) and the morphology of the heteronanostructure is barely unchanged as the reaction time increased to 20 h (Figure S2d), but the content of ZnSe was increased with 17.98% atomic percent of Se in EDX spectrum (Figure S2e), indicating that the longer the reaction time is, the more transformation of ZnO into ZnSe will have within a certain reaction time.

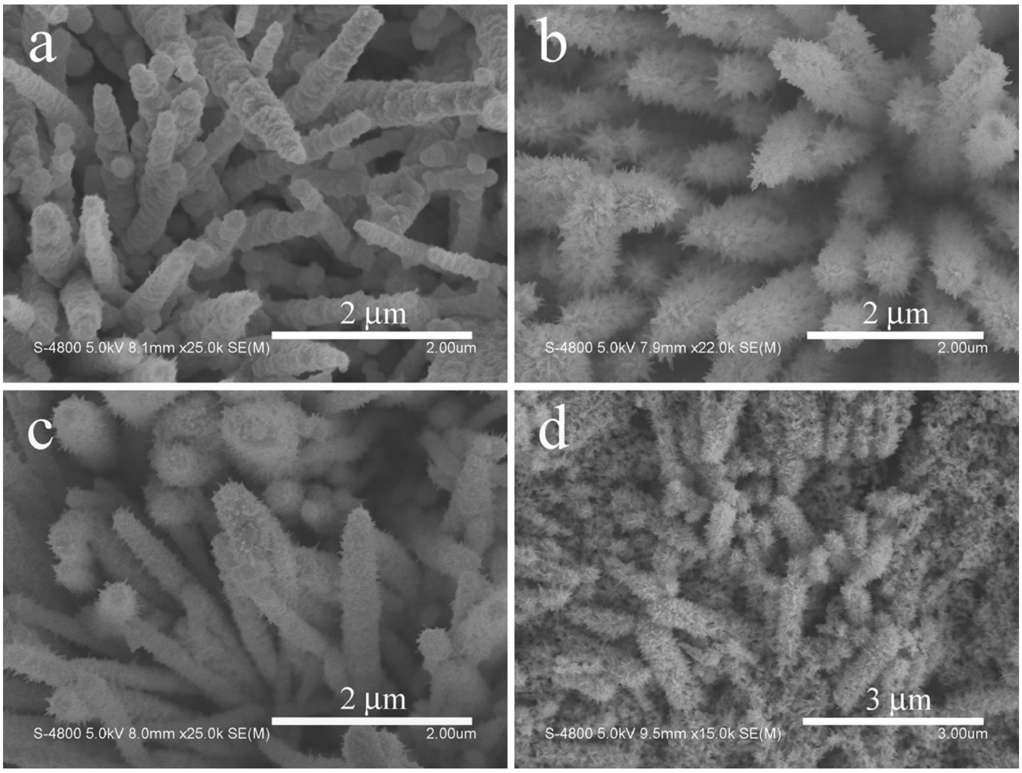

Figure S3. Typical FESEM images of the products synthesized with different concentration of $NaBH_4$ and reaction time as ammonia keeps constant of 15 mL. (a) without $NaBH_4$; (b) with 0.005 g of $NaBH_4$; (c) with 0.015 g of $NaBH_4$; and (d) with reaction time increased to 15 h.

The experimental results indicate that the microstructure of ZnSe shell is very sensitive to $NaBH_4$ concentration. Only ZnSe nanoparticles on ZnO-NRs were formed in the absence of $NaBH_4$ (Figure S3a), but similar nanorods structure was acquired with 0.005 g of $NaBH_4$ (Figure S3b). However, as the amount of $NaBH_4$ was increased to 0.015 g, the secondary ZnSe nanorods covered on ZnO-NRs became shorter (Figure S3c). The results demonstrated the concentration of $NaBH_4$ was critical for the formation of ZnSe nanorods shell, which is related with its adjustment on Se^{2-} ions concentration for the nucleation and growth of ZnSe seeds. Prolonging the reaction time to 15 h results in the product with most ZnO cores dissolved and some ZnSe nanorods shells collapsed (Figure S3d), due to etching of the excess ammonia with further aging.

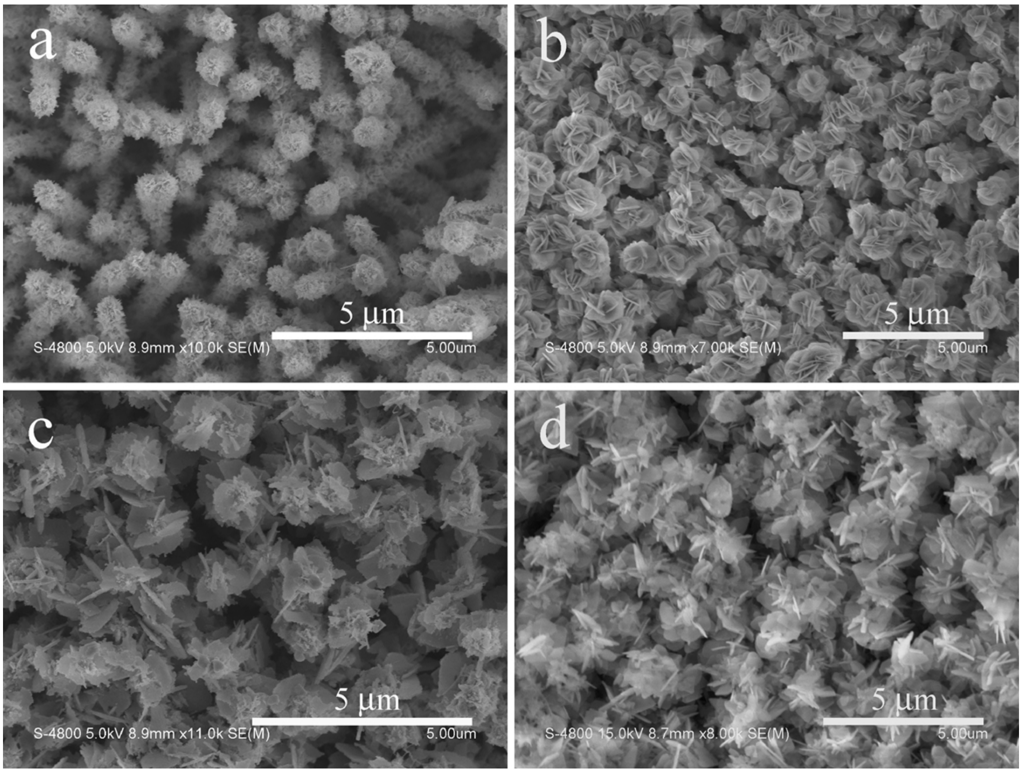

Figure S4. Typical FESEM images of the ZnO-NRs/ZnSe-NSs precursor array synthesized with different concentration of $NaBH_4$ and reaction time as ammonia keeps constant of 20 mL. (a) without $NaBH_4$; (b) with 0.005 g of $NaBH_4$; (c) with 0.015 g of $NaBH_4$; and (d) with reaction time increased to 15 h.

Variation of the $NaBH_4$ concentration found the product was dense nanorods accompanied by a small quantity of nanosheet-like structure on ZnO-NRs with no $NaBH_4$ (Figure S4a). While similar nanosheet-like shell was acquired with 0.005 g of $NaBH_4$ (Figure S4b), and the shell with nanosheets mixed with some nanoparticles was gained with 0.015 g of $NaBH_4$ (Figure S4c). The results indicated the suitable amount of $NaBH_4$ is necessary to generate the elegant ZnSe nanosheet-like precursor, which is relevant to its adjustment on Se^{2-} ions concentration for the growth and assembly of ZnSe seeds. In addition, increasing the reaction time to 15 h leads to scatter of some nanosheets shell (Figure S4d), due to the dissolution of ZnO nanorods cores by etching of ammonia.

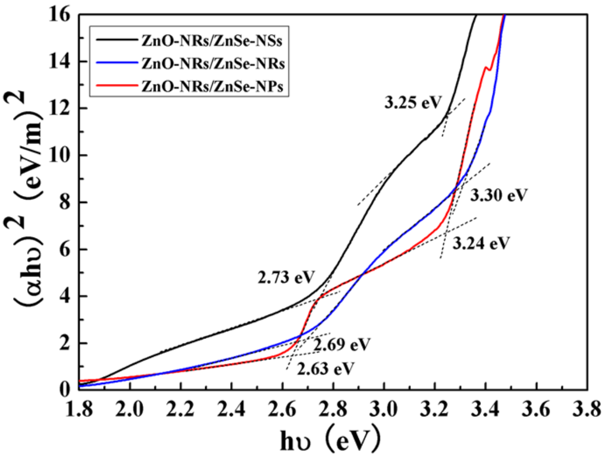

Figure S5. Tauc plots of three ZnO-NRs/ZnSe heteronanostructures.

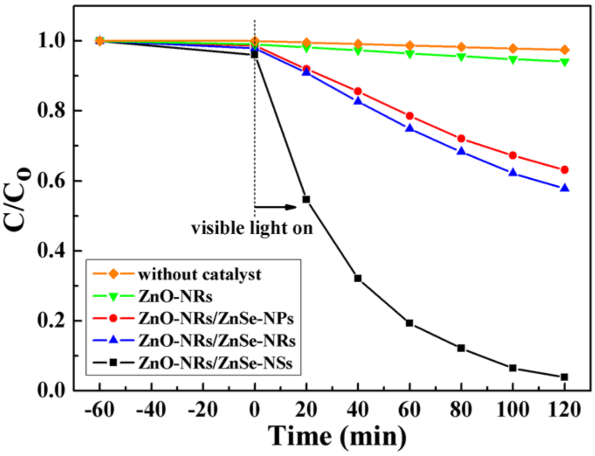

Figure S6. Comparison of RhB photodegradation without catalyst, with same mass of ZnO-NRs array and three different ZnO-NRs/ZnSe heteronanostructure arrays.

To compare the photocatalytic degradation of the materials with same mass, the control experiments have been conducted taking the mass of the ZnO-NRs/ZnSe-NSs heterostructure sample as a standard (0.23 mg), which was obtained by scratching the foil and measuring the powder, adjusting the sizes of the foils covered with other samples to make them with same mass of products according to the mass per footprint area also obtained by scratching the foil and measuring the powder. It revealed the ZnO-NRs and three ZnO-NRs/ZnSe heteronanostructures all can adsorb some RhB molecules, of which the differences are mainly due to the different surface areas of the products. The photocatalytic degradation rate of RhB was 41.0% with ZnO-NRs/ZnSe-NRs, 36.0% with ZnO-NRs/ZnSe-NPs, 4.9% with ZnO-NRs as well as 96.0% with ZnO-NRs/ZnSe-NSs. Clearly, the ZnO-NRs/ZnSe-NSs heterostructure array has better photocatalytic performance than that of the other two heteronanostructures, which is probably due to the larger surface area and more surface active reactive sites for photocatalytic reactions.

Compared with the data in Figure 7b using same footprint area of the foil, the variation of the data in Figure S6 comes from the mass differences after the selenization conversion. The mass of ZnO-NRs/ZnSe-NPs on the foil was slight increased compared with that of ZnO-NRs, but the mass of the

ZnO-NRs/ZnSe-NRs and ZnO-NRs/ZnSe-NSs, especially ZnO-NRS/ZnSe-NSs was obviously decreased due to dissolution of some ZnO nanorods at high concentration of ammonia.

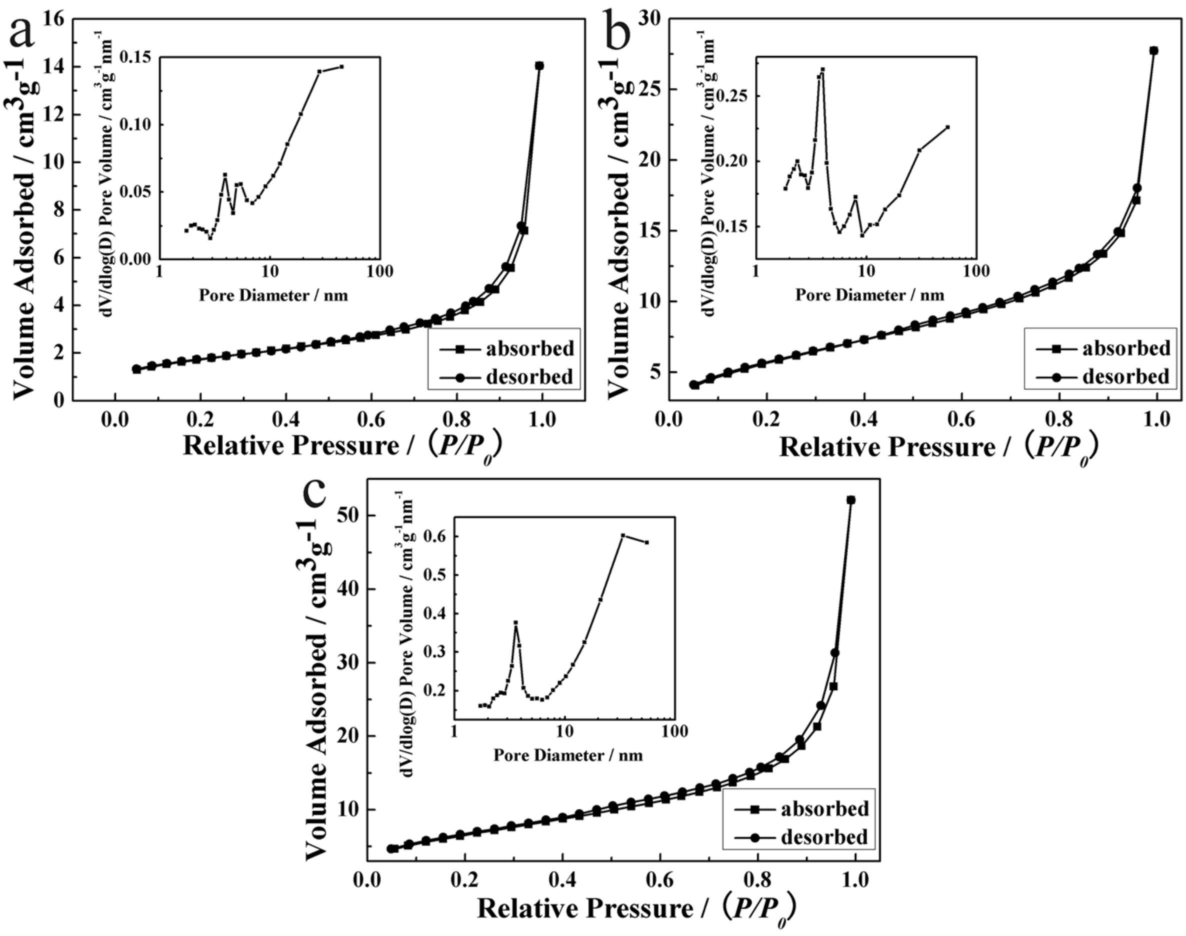

Figure S7. Nitrogen adsorption-desorption isotherms of the ZnO-NRs/ZnSe heteronanostructure samples. (a) ZnO-NRs/ZnSe-NPs; (b) ZnO-NRs/ZnSe-NRs; and (c) ZnO-NRs/ZnSe-NSs. The insets are their BJH pore-size distribution curves, respectively.

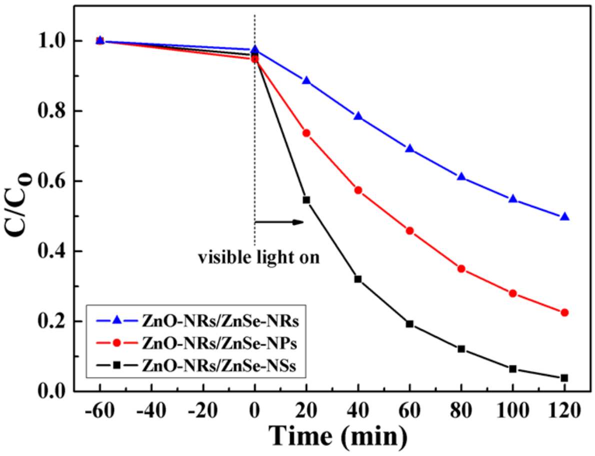

Figure S8. Comparison of RhB photodegradation with the same surface areas of three different ZnO-NRs/ZnSe heteronanostructure arrays (with 0.91 mg of ZnO-NRs/ZnSe-NPs, 0.27 mg of ZnO-NRs/ZnSe-NRs and 0.23 mg of ZnO-NRs/ZnSe-NSs by adjusting the size of the foil.).

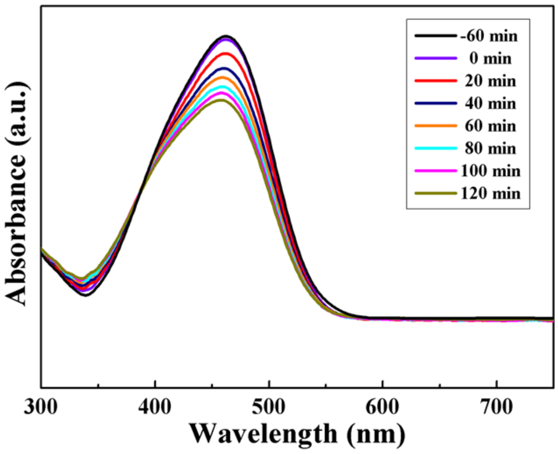

Figure S9. UV-visible absorption spectra of photodegradation MO aqueous solution with ZnO-NRs/ZnSe-NSs heterostructure array.

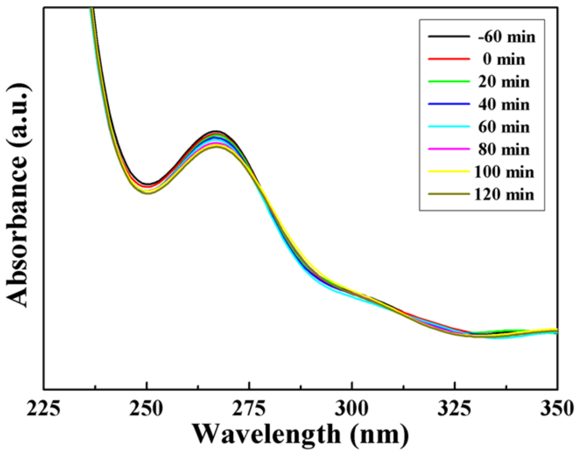

Figure S10. UV-visible absorption spectra of photodegradation phenol aqueous solution with ZnO-NRs/ZnSe-NSs heterostructure array.

Table S1. Cycling results of photocatalytic degradation of RhB with ZnO-NRs/ZnSe-NSs heterostructure array

Cycle Number	1	2	3	4	5	6	7	8	9	10
Decoloration	96.0%	95.9%	95.8%	95.6%	95.4%	95.1%	94.8%	94.4%	94.0%	93.5%